Published in final edited form as:
Annu Rev Biochem. 2013 ; 82: 531–550. doi:10.1146/annurev-biochem-051110-133601.

Post-translational biosynthesis of the protein-derived cofactor tryptophan tryptophylquinone

Victor L. Davidson[*] and **Carrie M. Wilmot**[#]

[*]Burnett School of Biomedical Sciences, College of Medicine, University of Central Florida, Orlando, FL 32827, U.S.A.

[#]Department of Biochemistry, Molecular Biology and Biophysics, University of Minnesota, Minneapolis, MN 55455, U.S.A. wilmo004@umn.edu.

Abstract

Methylamine dehydrogenase (MADH) catalyzes the oxidative deamination of methylamine to formaldehyde and ammonia. Tryptophan tryptophylquinone (TTQ) is the protein-derived cofactor of MADH that is required for these catalytic activities. TTQ is biosynthesized through the post-translational modification of two Trp residues within MADH, during which the indole rings of two Trp side chains are cross-linked and two oxygen atoms are inserted into one of the indole rings. MauG is a *c*-type diheme enzyme that catalyzes the final three reactions in TTQ formation. In total, this is a six-electron oxidation process requiring three cycles of MauG-dependent two-electron oxidation events using either H_2O_2 or O_2. The MauG redox form that is responsible for the catalytic activity is an unprecedented *bis*-Fe(IV) species. The amino acids of MADH that are modified are ~ 40 Å from the site where MauG binds oxygen, and the reaction proceeds by a hole hopping electron transfer mechanism. This review will address these highly unusual aspects of the long range catalytic reaction that is mediated by MauG.

Keywords

heme enzyme; high-valent iron; electron transfer; hole hopping

1. Introduction

Many enzymes are initially synthesized as an inactive form that requires an exogenous cofactor for activity. Only after the inactive apoprotein combines with the cofactor does it become active holoenzyme. A cofactor may be a metal (e.g., iron), an organic compound (e.g., flavin), or an organometallic compound (e.g., heme). These exogenous cofactors may be dissociable, tightly or covalently bound. However, there are a number of enzymes that have evolved an alternative method to introduce new catalytic functional groups into their active sites, circumventing the need for exogenous cofactors. These enzymes utilize protein-derived cofactors, which are catalytic or redox-active centers that are formed by post-translational modification of one or more amino acid residues (1, 2). These types of post-

Corresponding author: Victor L. Davidson, Burnett School of Biomedical Sciences, College of Medicine, University of Central Florida, 6900 Lake Nona Blvd., Orlando, FL 32827. Phone: 407-266-7111. victor.davidson@ucf.edu..

translational modifications are different from the more widely recognized modifications that primarily serve to regulate the biological activity of the protein or its localization (e.g., phosphorylation, methylation, glycosylation, prenylation, and cleavage of a signal or localization pre-sequence). Protein-derived cofactors are irreversible chemical modifications that include oxygenation of residues, peptide cyclization, side-chain dehydration, cross-linking of residues and internal proteolytic cleavage. These cofactors typically function at the enzyme active site, either by altering active site electrophilicity or by stabilizing free radical intermediates.

1.1 Methylamine dehydrogenase

Methylamine dehydrogenase (MADH) (3) catalyzes the oxidative deamination of methylamine to formaldehyde and ammonia, and transfers two electrons from the substrate to amicyanin, a type 1 copper protein (4). In doing so, MADH allows the host organism to use methylamine as a sole source of carbon, nitrogen and energy. Both MADH and amicyanin are localized in the periplasmic space of the bacterium. MADH catalysis requires the protein-derived cofactor tryptophan tryptophylquinone (TTQ; Figure 1) (5). The enzyme is a heterodimer of two 45 kDa α subunits, and two 14 kDa β subunits that each possess a TTQ (6) (Figure 2). TTQ is critical for both the catalytic and redox properties of MADH, as it performs active site chemistry and physically bridges this to surface mediated electron transfer to amicyanin. Crystal structures have been determined of MADH alone (6), MADH in complex with amicyanin (7), and MADH in complex with amicyanin and cytochrome *c*-551i (8), the electron acceptor of amicyanin (9).

1.2. Quinone cofactors generated by post-translational modification of enzyme active sites

TTQ is not the only quinone cofactor formed through post-translational modification of enzyme active site residues. Some of the best characterized protein-derived cofactors are quinone derivatives of tyrosine or tryptophan residues (Figure 1). Tyrosine-derived quinone cofactors have been found in oxidases from bacterial, mammalian and plant sources (10). Topaquinone (2,4,5-trihydroxyphenylalanine quinone, or TPQ) (11) is the protein-derived cofactor of the copper amine oxidases, which utilize a wide range of substrates and are involved in diverse physiological functions (12). The biosynthesis of TPQ requires the insertion of two oxygens into a specific tyrosine residue, and has been shown to be a self-processing event that is O_2 and copper-dependent (13, 14). Lysine tryptophylquinone (LTQ) is the protein-derived cofactor of mammalian lysyl oxidase, the key enzyme in cross-linking of elastin and collagen within connective tissue (15). Like TPQ, LTQ is a self-processed cofactor requiring copper and O_2, in which one atom of oxygen is incorporated into the tyrosine ring, and a covalent bond is formed between the C5 carbon of the tyrosine ring and the side chain nitrogen of a lysine residue (16, 17).

Tryptophan tryptophylquinone (TTQ) (5) and cysteine tryptophylquinone (CTQ) (18-20) are the protein-derived cofactors of two distinct classes of amine dehydrogenases. TTQ is formed by post-translational modification of two tryptophan residues of the polypeptide chain. Two atoms of oxygen are incorporated into the indole ring of one Trp, and a covalent bond between the indole rings cross-links the two Trp residues. CTQ differs in that the tryptophylquinone is cross-linked with Cys through a thioether bond rather than another Trp.

In contrast to the TPQ and LTQ cofactors, the biosynthesis of TTQ is not a self-processing event, but requires the action of at least one other enzyme. This review will focus on MADH from *Paracoccus denitrificans*, where an unusual diheme enzyme, MauG (21), plays a role in catalyzing the post-translational modifications that yield TTQ. As discussed in this review, MauG-dependent TTQ biosynthesis involves a previously uncharacterized mechanism for oxygen activation, and remote mechanism of enzyme catalysis in which long range electron transfer is required for the radical-mediated catalytic reactions.

2. General features of MADH biogenesis

2.1. The methylamine utilization gene cluster and MauG expression

The biogenesis of MADH requires not only the post-translational modifications to generate TTQ, but also formation of six disulfide bonds in the β subunit, export of subunits to the periplasm, and their assembly into the $\alpha_2\beta_2$ quaternary structure. The genes encoding the α and β subunits of MADH are located in the methylamine utilization (*mau*) gene cluster (22). The *mau* cluster of *P. denitrificans* has 11 genes with a gene order of *mauRFBEDACJGMN* (Figure 3) (23). The α and β subunits of MADH are encoded by *mauB* and *mauA*, respectively, and *mauC* (24) encodes amicyanin. Four other genes were shown to be essential for MADH biogenesis in *P. denitrificans*. Deletions of either *mauF* (25), *mauD* (26), *mauE* (26) or *mauG* (23) result in loss of MADH activity and the ability of the bacterium to grow on methylamine. In the first three deletions, no MADH β subunit could be detected in cell extracts, and the levels of MADH α subunit were significantly decreased. However, while cells with the *mauG* deletion are lacking in MADH activity and unable to grow on methylamine, it was shown by Western blot analysis that near wild-type levels of the MADH α and β subunits are expressed (23). This suggested that MauG might play a role in TTQ formation.

The sequence of *mauG* contains two CXXCH *c*-type heme binding motifs in which the Cys residues form thioether bonds that covalently attach the heme to the protein, with the His acting as an axial ligand to the iron. While *c*-type hemes typically mediate electron transfer, they can also catalyze oxidative chemistry. When *P. denitrificans* is grown with methylamine as the sole carbon source, the cells are induced to produce large amounts of MADH and amicyanin (4, 27). However, the MauG protein has never been detected in extracts of these cells, consistent with it being involved in a maturation event. A recombinant MauG was isolated and purified after homologous expression of *mauG* in *P. denitrificans* (21). MauG was shown to be a 42.3 kDa monomer that does possess two covalently bound *c*-type hemes, as predicted from the gene sequence (21).

In order to precisely determine the role of MauG in TTQ biosynthesis, a recombinant expression system for MADH was developed (28). A plasmid containing *mauFBEDACJG,* which includes the MADH structural genes and those required for MADH biogenesis, was placed in *Rhodobacter sphaeroides*, a bacterium that does not produce MADH. Active recombinant MADH, with the correctly synthesized TTQ cofactor, was isolated from these cells. The *mauG* gene was then inactivated in this expression system with the hope that this would result in accumulation of the natural substrate for the *mauG* gene product, MauG. The substrate protein isolated from the periplasm is a $\alpha_2\beta_2$ heterodimeric MADH protein that is

inactive towards methylamine and lacks the visible absorption spectrum characteristic of the TTQ cofactor. Analysis of this biosynthetic intermediate of MADH by proteolysis and mass spectrometry reveals that βTrp57 is monohydroxylated and that the covalent cross-link to residue βTrp108 has not been formed (29). Using $^{18}O_2$ labeling studies it was determined that the biosynthetic MADH intermediate is hydroxylated at the C7 position of βTrp57, and thus insertion of the second oxygen must be at the C6 position (30). This species is designated preMADH. In order to demonstrate that preMADH was indeed the substrate for MauG, it was incubated in vitro with purified MauG and oxidation equivalents provided either by O_2 plus an electron donor, or by H_2O_2 (31). This resulted in completion of TTQ biosynthesis and formation of active MADH. Thus, while the mechanism by which the first oxygen is inserted into residue βTrp57 remains to be elucidated, these results demonstrate that the final steps of TTQ biosynthesis are catalyzed by MauG.

2.3. Steady-state assays of MauG-dependent TTQ biosynthesis

Steady-state kinetic studies have exploited the fact that the preMADH substrate has no visible absorption, whereas the mature TTQ cofactor does. As TTQ is a two-electron redox cofactor, it can assume three different redox states. The oxidized quinone exhibits a broad absorbance centered at 440 nm, the one-electron reduced semiquinone exhibits an absorption maximum at 428 nm, and the two-electron reduced quinol exhibits an absorption maximum at 330 nm (32). When diferric MauG was incubated with excess preMADH, and the reaction initiated by addition of oxidizing equivalents [O], either as a reductant plus O_2 or as H_2O_2, an increase in absorbance centered on 440 nm was observed (33, 34). This corresponds to the steady- state formation of the fully oxidized quinone form of TTQ in MADH (Figure 4A). The reaction exhibits a k_{cat} of 0.2 s^{-1} and a K_m of 6.6 μM. Upon reaction completion, the product was shown to possess MADH activity through addition of methylamine to the reaction mixture that caused disappearance of the quinone peak at 440 nm and appearance of a quinol peak at 330 nm, as expected for substrate reduction of mature TTQ-containing MADH in the absence of amicyanin.

A transient intermediate with a λ_{max} at 330 nm was observed early in the steady-state TTQ biosynthesis reaction with preMADH as a substrate (34). From this spectral feature, it was postulated that the quinol form of TTQ was an intermediate in TTQ biosynthesis from preMADH. To test this hypothesis, quinol MADH was formed in vitro by reduction with dithionite, and then tested as a substrate for MauG. Quinol MADH was not oxidized by H_2O_2 alone, but in the presence of MauG, H_2O_2-dependent oxidation of the quinol to TTQ was observed, suggesting that this is likely the final step in TTQ biosynthesis in vivo. In light of these observations, a second steady-state assay was established that used quinol MADH as a substrate (35) (Figure 4B). Since quinol MADH lacks absorbance at 440 nm, the formation of product could again be monitored by the appearance of the peak at this wavelength. This reaction exhibited a k_{cat} of 4.2 s^{-1} and a K_m of 11.1 μM.

Given this knowledge, it is possible to propose two alternative chemical routes for MauG-dependent TTQ biosynthesis (Figure 5). This model has provided a framework for the design of experiments to elucidate the precise kinetic and chemical mechanism for TTQ biosynthesis.

3. Spectroscopic and redox properties of MauG

In order to understand the mechanism by which MauG is able to catalyze the complex six-electron oxidation required for TTQ biosynthesis, it is necessary to fully understand its redox properties. The visible absorption spectra of diferric and diferrous MauG are typical of those of *c*-type cytochromes (Figure 6A). In contrast, the electron paramagnetic resonance (EPR) spectra of the ferric hemes of oxidized MauG are atypical of *c*-type cytochromes (21). One heme exhibits a high-spin heme EPR signal that is similar to those of myoglobin and the heme oxygenase-heme complex. The other heme exhibits a low-spin heme EPR signal that is similar to those of complexes of cytochrome P450cam with an exogenous axial sixth ligand. Resonance Raman spectroscopy of MauG also indicated the presence of a low-spin six-coordinate heme and a high-spin five-coordinate heme in both the diferric and diferrous states (36).

Redox titrations of MauG demonstrated that the two hemes were simultaneously reduced and oxidized rather than sequentially. This indicates that the intrinsic oxidation-reduction midpoint potential (E_m) values for the Fe(III)/Fe(II) couple of each of the two hemes are equivalent. MauG exhibits two E_m values of -159 and -254 mV (36) for the inter-conversion between diferric and diferrous states, which correspond to the sequential addition or removal of the first and second electrons from the diheme system. This was described as negative redox cooperativity, and indicates that facile equilibration of electrons occurs between the two hemes. From a catalytic standpoint, this means MauG contains a diheme two-electron redox cofactor, rather than two independent hemes.

It is evident from the nature of the chemistry catalyzed by MauG that the reaction mechanism requires the generation of a high-valent iron species to drive the oxygenation and cross-linking reactions required for TTQ formation. Heme-containing oxygenases and peroxidases often use a high-valent Fe intermediate known as Compound I, which is a ferryl species (i.e., Fe(IV)=O) coupled to a π-cation radical located on the porphyrin ring. Compound ES is a variation of Compound I, in which the Fe(IV)=O heme is coupled to an amino acid-based cation radical in close proximity to the heme. MauG displays a new natural strategy for stabilizing an Fe(V)-equivalent within a protein through utilization of a previously undescribed *bis*-Fe(IV) redox state (37). This redox state can be formed either by addition of O_2 to diferrous MauG, or addition of H_2O_2 to diferric MauG (38). It is unknown whether O_2 or H_2O_2 is the physiological oxidant, however the same *bis*-Fe(IV) product results from either, and for quantitative control, H_2O_2 has been the preferred method for generating the *bis*-Fe(IV) state. When diferric MauG is mixed with excess H_2O_2 the reaction is complete within the dead time of mixing (i.e., $k > 300\ s^{-1}$) (38). The absorption spectrum of this redox form exhibits a decrease in intensity of the Soret peak of MauG relative to the diferric spectrum and a shift in its maximum from 405 to 407 nm (Figure 6B). As expected for two Fe(IV) hemes, the EPR spectrum of this intermediate is EPR-silent (37). Mössbauer spectroscopy of this intermediate revealed the presence of two distinct Fe(IV) species (37). One was consistent with an Fe(IV)=O species ($\delta = 0.06$ mm/s, $\Delta E_Q = 1.70$ mm/s). The other was assigned to a unprecedented Fe(IV) species with two axial ligands from protein ($\delta = 0.17$ mm/s, $\Delta E_Q = 2.54$ mm/s) (37). The *bis*-Fe(IV) species is relatively stable, as it spontaneously decays back to the diferric state over several minutes. Proof of the catalytic

competence of this *bis*-Fe(IV) intermediate was demonstrated by mixing this species with preMADH (37). This results in rapid return of MauG to the diferric state, as judged by UV-vis absorbance and EPR spectroscopy. A new organic radical EPR signal is present after the reaction, which was shown to be on preMADH (37). This demonstrated that the initial reaction in MauG-dependent TTQ biosynthesis involves oxidation of amino acid residues on preMADH.

4. Structure-function studies of MauG and preMADH

4.1. Structure of MauG

Although MauG alone has not been crystallized, the X-ray crystal structure of its complex with the preMADH substrate has been determined to 2.1 Å resolution (39). MauG contains two protein domains, each containing one of the hemes (Figure 7A). Both hemes of MauG have the expected proximal axial His ligand (His35 and His205, respectively) from the *c*-type heme sequence motif CXXCH. The two domains are topologically equivalent, and likely arose through a gene duplication event. The N-terminal domain heme, which is furthest from preMADH in the complex, has an open coordination site and a distal pocket that is solvent accessible. As it is five-coordinate, this makes it the spectroscopically characterized high-spin heme (21). The coordination of the C-terminal domain heme, which lies closest to the preMADH interface, is completed by a tyrosine (Tyr294) identifying it as the low-spin heme. Tyrosine is relatively rare as a heme ligand, and this is the first example involving a *c*-type heme. This heme is more sequestered from solvent than the high-spin heme, and spectroscopic studies are consistent with retention of the His-Tyr ligation in all three MauG redox states (21, 36, 37, 40). At the MauG domain interface between the hemes lies a conserved tryptophan (Trp93). A calcium ion is also bound between the domains, and is ligated by four water molecules and two amino acids that are strictly conserved (side-chain of Asn66 and main-chain carbonyl of Pro277) (41).

4.2. Long range MauG-dependent TTQ biosynthesis in crystallo

The structure of preMADH is essentially identical to that of mature MADH, with differences localized to the preTTQ site. MauG binds at the same site on MADH as amicyanin, the physiological electron acceptor for methylamine turnover (7). While there is no homology between amicyanin and MauG, they are similar in that amicyanin accepts electrons from the reduced and semiquinone forms of TTQ during catalysis and MauG accepts electrons from preTTQ during biosynthesis. Prior to the structure, it was hypothesized that MauG catalysis involved a heme-generated reactive oxygen species that directly attacked the C6 of preTTQ. So it was a surprise when the structure revealed that neither MauG heme is in direct contact with preMADH (Figure 7B). In addition, the preTTQ residues are not at the preMADH surface, but buried and in a similar position to those of mature TTQ. In fact, the through-space distances are substantial: the MauG heme porphyrin nearest to the interface with preMADH is 15.5 Å to the closest preTTQ atom, and separated from the other MauG porphyrin by 14.5 Å.

The catalytic relevance of this structure was demonstrated through addition of H_2O_2 to the MauG-preMADH crystals that led to TTQ formation in crystallo (Figure 7C). The structure

has a number of ramifications: (i) there are no significant conformational changes during MauG turnover, (ii) the reaction is processive, and does not require dissociation of the complex between each two-electron oxidation event, (iii) the reaction involves long range electron transfer, (iv) the oxygen inserted into preTTQ at C6 is likely solvent-derived, and (v) the same amino acids and chemical environment in (pre)MADH support two very different chemistries; conversion of preTTQ to TTQ and mature MADH amine dehydrogenase activity. This latter point is interesting in a broader evolutionary sense, as it suggests that a protein environment which supports the synthesis of Tyr and Trp-derived quinone cofactors is inherently conducive to the oxidation of primary amines to aldehydes following cofactor formation. Currently, there are four enzymes known to have independently evolved this linked chemistry: MADH and its homologs, quinohemoprotein amine dehydrogenase, copper amine oxidase and lysyl oxidase, whose cofactors were discussed earlier (see Figure 1).

4.3. The distal pocket of the high-spin five-coordinate heme of MauG

The crystal structure of MauG identified a number of conserved residues in the distal pocket of the high-spin five-coordinate heme; Gln103, Pro107 and Glu113 (Figure 8) (39). X-ray absorption spectroscopy of H_2O_2 treated MauG coupled to density functional theory modeling demonstrated that the high-spin heme is the site of the Fe(IV)=O in *bis*-Fe(IV) MauG (40). This is also consistent with electron density observed in H_2O_2 treated MauG-preMADH crystals (39). Therefore, this is the heme that reacts with H_2O_2 or O_2. Addition of NO to diferrous MauG also shows exclusive binding to the high-spin heme, as demonstrated in solution by EPR spectroscopy (42) and in crystallo through addition of NO to diferrous MauG-preMADH crystals (Figure 8) (43). Based on the NO-MauG-preMADH crystal structure, Glu113 may be important in promoting cleavage of the O–O bond through protonation of oxygen intermediates bound to heme. The structure suggests that Gln103 may be important in stabilizing the Fe(IV)=O by hydrogen bonding to the oxo, and is consistent with a quantum chemical investigation that explored the unusual Mössbauer spectroscopic parameters of the *bis*-Fe(IV) MauG (44). For the assigned Fe(IV)=O species, the ΔE_Q value of 1.70 mm/s lies between the average experimental ΔE_Q values in heme proteins for protonated and unprotonated forms. The model that best fit the observed parameters suggested that the Fe(IV)=O species is stabilized by a hydrogen bond to an active site residue, which based on the NO-MauG adduct crystal structure is likely Gln103, and this would account for the ΔE_Q value lying between the average experimental ΔE_Q values of the different protonated states.

Perhaps the most intriguing conserved residue is Pro107, which has been suggested to keep the site primed for H_2O_2 binding and O_2 activation (39). The residue changes conformation from upPro to downPro (45) upon binding of NO, and helps position the distal atom of NO so that it points towards Glu113, consistent with the proposal that Glu113 may play an acid / base role in *bis*-Fe(IV) formation. Pro107 has been mutated to Val, Ser and Cys (46). P107C is inactive, and the crystal structure and mass spectrometry show that Cys107 has been oxidized to sulfinic acid and become a heme ligand. The P107V MauG-preMADH crystal structure shows that P107V leads to minimal structural perturbations in the distal pocket, and the mutant has a similar catalytic activity to wild-type MauG, with k_{cat} =0.10 s^{-1} and

K_m=1.3 μM. However, the P107V MauG enzyme is more susceptible to oxidative damage than wild-type, suggesting that the rigidity of Pro may be important in controlling reactive oxygen species at the high-spin heme. Surprisingly, the P107S MauG-preMADH crystal structure shows that Glu113 has moved 3.1 Å into the distal pocket so that it is now coordinated to the heme. This mutant is inactive in TTQ biosynthesis, and the K_d for H_2O_2 increases by at least 1000-fold, presumably because of Glu113 blocking access to the heme. The P107S variant is even more susceptible to protein oxidation than P107V following reaction with H_2O_2, including evidence of heme degradation, further underscoring the role of Pro107 in protecting MauG from oxidative damage.

4.4. The role of calcium in MauG

The crystal structure of the MauG-preMADH complex reveals the presence of a Ca^{2+} in proximity to the two hemes, connecting to both via hydrogen bond networks (see Figure 7A). This Ca^{2+} does not readily dissociate from MauG; however after Ca^{2+} removal by extensive treatment with chelators, MauG is no longer able to catalyze TTQ biosynthesis and exhibits altered absorption, resonance Raman and EPR spectra (41, 47). The circular dichroism spectra of native and Ca^{2+}-depleted MauG are essentially the same, consistent with Ca^{2+}-induced conformational changes involving domain or loop movements rather than general unfolding or alteration of secondary structure. This is consistent with the crystal structure, in which the Ca^{2+} is bound between the N- and C-terminal domains. Increased domain dynamics is also suggested by the fact that it has not been possible to crystallize the Ca^{2+}-depleted MauG. However, spectroscopic studies have given insight into the effect Ca^{2+} has on the structure. Addition of H_2O_2 to the Ca^{2+}-depleted MauG did not yield spectral changes characteristic of formation of the *bis*-Fe(IV) state, as seen for native MauG. Removal of Ca^{2+} alters the EPR signals of each ferric heme, such that the intensity of the high-spin heme is decreased and the low-spin heme is significantly broadened. It was shown that in the Ca^{2+}-depleted MauG the original high-spin heme is converted to low-spin, and the original low-spin heme exhibits a change in relative orientations of its two axial ligands. EPR and Mössbauer spectroscopic results (47) show that the two hemes are present as unusual highly axial low-spin (HALS)-like hemes (48, 49) in Ca^{2+}-depleted MauG, with a smaller orientation angle between the two axial ligand planes. The effects of Ca^{2+}-depletion are completely reversible. After addition of Ca^{2+} to the Ca^{2+}-depleted MauG, full TTQ biosynthesis activity and reactivity towards H_2O_2 is restored, and the spectral properties return to those of native MauG. Kinetic and equilibrium studies of Ca^{2+} binding to Ca^{2+}-depleted MauG indicates a two-step mechanism, where Ca^{2+} initially reversibly binds to Ca^{2+}-depleted MauG, followed by a relatively slow, but highly favorable, conformational change, yielding an apparent equilibrium K_d value of 5.3 μM (41). These findings provide insight into the correlation of the enzyme activity with the orientation of axial heme ligands, and describe a role for the calcium ion in maintaining a structural orientation that is required for activity.

5. Role of MADH active site residues in the MauG-independent hydroxylation to form preMADH

Whereas MADH is an $\alpha_2\beta_2$ heterotetramer, the CTQ enzyme quinohemoprotein amine dehydrogenase is an $\alpha\beta\gamma$ trimer with no significant structural or sequence homology. However, the actives sites of the enzymes are very similar. Each has two spatially conserved Asp residues in the active site (50) (Figure 9). When the Asp residues in MADH were mutated to test their roles in MADH-dependent amine oxidation, barely detectable levels of inactive protein were obtained. Analysis by mass spectrometry revealed that mutation of MADH βAsp76 to Asn leads to protein with no βTrp57 or βTrp108 modifications at all, meaning that this residue is absolutely required for the first βTrp57 hydroxylation that occurs prior to MauG-catalyzed chemistry. When mutated to Asn, βAsp32 also affects the efficacy of the first βTrp57 hydroxylation, but does not significantly interfere with MauG-catalyzed chemistry, leading to a mix of unmodified and mature MADH upon expression. Although the mechanism by which the initial Trp hydroxylation occurs in MADH is currently unknown, these data suggest that the MADH active site structure plays a role in this initial modification of TTQ biosynthesis.

6. Electron transfer reactions between MauG, preMADH and MADH

Three single-turnover reactions have been described that involve MauG and preMADH or different redox forms of MADH (Figure 10, Table 1). In contrast to the steady-state reactions that monitored the rate of TTQ formation, these single-turnover reactions are electron transfer reactions monitored through the changes in the absorbance of MauG or MADH that are associated with changes in redox state.

6.1. The initial two-electron oxidation of preMADH

The initial two-electron oxidation of preMADH was studied by mixing preMADH with *bis*-Fe(IV) MauG, which was pre-formed by mixing with stoichiometric H_2O_2 (38) (Figure 10A). The reaction kinetics of this two-electron oxidation fit to a single exponential relaxation. This suggests a kinetic mechanism with a relatively slow one-electron transfer followed by a faster one-electron transfer. As such, no intermediate state accumulates. The observed rate in this case is that of the slower initial electron transfer event in which an electron is transferred to *bis*-Fe(IV) MauG from either Trp108 or OH-Trp57 of preMADH to generate a radical species. The subsequent faster electron transfer results in loss of a second electron from these Trps, likely generating a diradical species. The dependence of the observed rate of reaction on preMADH concentration exhibits saturation behavior, with a limiting first-order rate constant for the reaction of k_{lim} =0.80 s^{-1}, which is orders of magnitude faster than the spontaneous rate of decay to the diferric state. The K_d for complex formation is relatively low, and determined to be ≤1.5 μM (38). Identical values of k_{lim} and K_d were determined when the reaction was initiated by mixing the pre-formed complex of preMADH and diferric MauG with H_2O_2, identifying the MauG catalytic mechanism as random order. These results are in contrast to those typically observed with other enzymes that utilize high-valent heme species, such as Compound I, which undergo rapid spontaneous decay that can cause oxidative damage. For example, cytochrome P450

enzymes that utilize Compound I are unreactive toward oxygen until organic substrate binds, at which point the high-spin heme becomes capable of binding and activating O_2, leading to the high-valent species being directed towards productive catalytic chemistry (51). As the ferryl heme oxo group directly attacks organic substrate in this case, this would facilitate the evolution of an ordered mechanism. In contrast, the MauG ferryl heme is 40.1 Å from preTTQ, which likely favored the evolution of increased high-valent oxidant stability as a strategy to minimize oxidative damage.

While the presence or absence of preMADH has no influence on the reactivity of MauG towards oxidation equivalents, repeated formation of *bis*-Fe(IV) followed by spontaneous decay to the diferric state in the absence of preMADH leads to loss of catalytic activity (52). Mass spectrometric analysis of MauG after incubation with excess H_2O_2 provided evidence that oxidative damage had occurred (46). The radical scavenger hydroxyurea protects against inactivation, consistent with a free radical damage mechanism (52). Thus, the kinetic mechanisms, and mechanisms of avoidance and susceptibility to suicide inactivation exhibited by MauG, are distinct from those of other heme-dependent and non-heme Fe-dependent enzymes that activate O_2.

6.2. The two-electron oxidation of quinol MADH

To study the final two-electron oxidation step in TTQ biosynthesis, electron transfer from quinol MADH to *bis*-Fe(IV) MauG was characterized (Figure 10B). Quinol MADH was generated by stoichiometric reduction of native MADH by dithionite (53), and this was then mixed with pre-formed *bis*-Fe(IV) MauG. The resulting reaction exhibited a k_{lim} =20 s^{-1} and a K_d of 11.2 μM (35). Comparison of these results with those of the initial oxidation of preMADH, suggests that the initial two-electron oxidation of preMADH may be the rate-limiting step in the overall six-electron oxidation process (Table 1), as the rate constant for that reaction is much closer to the steady-state k_{cat} value than is the rate of this final two-electron oxidation. It is also noteworthy that the K_d value for the complex with quinol MADH is about ten-fold greater than that for the complex with preMADH. It is not surprising that quinol MADH dissociates from MauG more readily than does preMADH, as at this point the cofactor has been assembled and requires only oxidation to yield TTQ. Should release of quinol MADH from MauG occur in vivo prior to the final oxidation step, quinol MADH could alternatively be oxidized to the quinone by its natural electron acceptor amicyanin, as occurs in the catalytic cycle of mature MADH (4).

6.3. Electron transfer from diferrous MauG to quinone MADH

Single-turnover kinetics were used to study another electron transfer reaction, that from diferrous MauG to the oxidized TTQ of MADH (Figure 10C). This reaction is not involved in TTQ biosynthesis, but it is thermodynamically favorable and may be monitored spectroscopically (35). The reaction exhibits a k_{lim} =0.07 s^{-1} and a K_d of 10.1 μM. The similarity of this K_d value to that for the quinol MADH and *bis*-Fe(IV) MauG reaction, which is much greater than that for the MauG-preMADH complex, indicates that the extent of TTQ maturity rather than its redox state is a major determinant in the affinity of MauG towards different forms of MADH. As this reaction does not involve the formation of the *bis*-Fe(IV) species, the ability to monitor this reaction has proven to be a useful tool in

separating mutations of MauG residues that destabilize the *bis*-Fe(IV) state from those that disrupt electron transfer between the two proteins (discussed later).

7. The importance of Tyr294 of MauG to the *bis*-Fe(IV) redox state

MauG is the first example of a *c*-type heme with axial ligation by tyrosine, and Tyr294 is a conserved residue in the known MauG sequences (39). This heme is also the first example of a protein-bound heme that is able to stabilize an Fe(IV) state without an exogenous ligand. Quantum chemical modeling indicates that the His-Tyr ligand set determines the unusually large Mössbauer ΔE_Q parameter of the Fe(IV) heme (ΔE_Q = 2.54 mm/s) (37, 44). To probe the significance of Tyr294, it was replaced with His by site-directed mutagenesis (54). The crystal structure of Y294H MauG-preMADH shows that the heme now has His-His axial ligation, and functional analysis indicates that this variant is unable to catalyze TTQ biosynthesis.

Several results indicated that the mutation of the Tyr294 axial ligand affects not only the properties of that heme, but also those of the five-coordinate heme, despite the fact that the two heme irons are separated by 21 Å. The Y294H mutation causes significant changes to both E_m values, −17 mV and −377 mV for Y294H MauG (54) compared to −158 mV and −246 mV for native MauG (36). Diferrous Y294H MauG binds CO, but with a K_d value that is 14-fold less than that for native diferrous MauG (54). Spectroscopic analysis of the reaction of Y294H MauG with H_2O_2 suggests that the six-coordinate His-His heme of Y294H MauG cannot stabilize an Fe(IV) state. Instead, after addition of H_2O_2 to Y294H MauG, an alternative Fe(V)-equivalent state forms with spectral features characteristic of an Fe(IV)=O with an accompanying π-cation radical present solely at the N-terminal heme (54).

It is proposed that a critical role of the *bis*-Fe(IV) state is not only to provide a strong oxidant, but to significantly shorten the distance required for the catalytic long range electron transfer from preTTQ (40.1 Å to the Fe(IV)=O compared to 15.4 Å to the Fe(IV) porphyrin of the six-coordinate heme). Similar to the *bis*-Fe(IV) redox state of wild-type MauG, this Compound I-like state of Y294H MauG is relatively stable. However, it does not react with preMADH, and Y294H MauG cannot catalyze TTQ biosynthesis from either preMADH or quinol MADH. In contrast, the non-physiological electron transfer reaction from diferrous Y294H MauG to quinone MADH, which is not involved in TTQ biosynthesis and does not require the *bis*-Fe(IV) state, is not negatively impacted by the mutation. The X-ray crystal structure of the Y294H MauG-preMADH complex shows that the inability to catalyze TTQ biosynthesis is not a consequence of significant alteration of the protein structure, the protein-protein interface, or the heme environment beyond the replacement of the Tyr axial ligand with His. Thus, the electron transfer path is operative, but generation of a high-valent state that is confined to the more distant N-terminal heme is not sufficient for MauG-dependent TTQ biosynthesis.

8. Tryptophan mediated hole hopping during the long range electron transfer required for TTQ biosynthesis

The importance of minimizing the distance for the long range electron transfer reactions required during MauG-dependent TTQ biosynthesis was highlighted by the study of Y294H MauG described above (54). However, the distance from preTTQ to the heme porphyrin of the six-coordinate heme (15.4 Å) is still rather long for efficient electron transfer. Furthermore, the rate of the electron transfer reaction from preMADH to *bis*-Fe(IV) MauG, which is believed to be approximately isoenergetic, is approximately ten-fold greater than the rate of the electron transfer reaction from diferrous MauG to quinone MADH, which is energetically favorable. Site-directed mutagenesis and kinetic and thermodynamic studies have demonstrated that the former reaction occurs via a hole hopping mechanism, while the latter occurs by a single-step electron tunneling mechanism (35). During long range electron tunneling through proteins, the amino acid residues that mediate electron transfer simply serve as a conduit, and do not undergo changes in redox states (55). In contrast, in a hopping mechanism certain intervening amino acid residues are reversibly oxidized and reduced, and serve as intermediate points in a multi-step process (56). In hole hopping, the electron acceptor oxidizes the intermediate, which in turn oxidizes the electron donor. This means that the electron that leaves the electron donor (in this case, preTTQ) is not the same as the electron that enters the electron acceptor (in this case, *bis*-Fe(IV) MauG), but an electron displaced from the intervening amino acid. This allows the overall electron transfer reaction to occur more rapidly than via single-step long range electron tunneling between donor and acceptor, as the rate of the slowest hop will be much faster than that for electron tunneling over the entire distance.

8.1. Identification of Trp199 of MauG as a hopping intermediate

Residue Trp199 of MauG resides at the MauG-preMADH interface, and is positioned midway between the residues that are modified and the nearest heme (see Figure 7B). It was postulated that Trp199 could be reversibly oxidized and reduced, thus serving as a hopping intermediate between preTTQ and the Fe(IV) His-Tyr ligated heme. The idea of Trp199-mediated hole hopping during electron transfer was tested by site-directed mutagenesis (57). Mutations of Trp199 do not affect the spectroscopic and redox properties of MauG, nor its ability to stabilize the *bis*-Fe(IV) state. Crystal structures of complexes of these MauG variants with preMADH show no significant perturbation of the MauG-preMADH structure or protein interface. However, the MauG variants are not able to synthesize TTQ from preMADH. In contrast, the electron transfer reaction from diferrous MauG to quinone MADH that does not involve the *bis*-Fe(IV) intermediate, and is believed to occur via single-step electron tunneling, is minimally affected by the mutations.

8.2. Characterization of tunneling and hopping reactions through MauG using electron transfer theory

The dependence on temperature of the rates of electron transfer from diferrous MauG to quinone MADH and from preMADH to *bis*-Fe(IV) MauG were analyzed by Marcus theory and compared (58). While these reactions occur over the same distance, analysis of the two

reactions yielded different values of electronic coupling and electron transfer distance. The experimentally-determined distance for the reaction from diferrous MauG to quinone MADH matched the distance in the crystal structure between TTQ and the nearest heme of MauG. In contrast, the experimentally-determined distance for the reaction from preMADH to *bis*-Fe(IV) MauG was much shorter, being consistent with the distance from Trp199 to either the nearest heme or the residues on preMADH that form TTQ and a hopping mechanism. These results together with those of the site-directed mutagenesis study show that Trp199 plays a critical role in mediating hole hopping from preMADH to *bis*-Fe(IV) MauG during the long range electron transfer required for TTQ biosynthesis.

8.3. Does Trp93 also mediate hopping during electron transfer between hemes?

The hemes of MauG function as a diheme system rather than two independent hemes, despite their physical separation (36, 37). This suggests that the strictly conserved Trp93, which resides midway between the hemes (see Figure 7A), may mediate electron transfer between them. It has not been possible to directly measure the rate of this reaction, or to generate mutants of Trp93 that can be used to directly address this issue. However, it was noted that the EPR spectrum of the *bis*-Fe(IV) MauG, while primarily EPR silent, did display a signal that was attributed to an organic radical which represented about 1% of the protein (37). This was proposed to be a cation radical in equilibrium with the two hemes in the high-valent state. This observation is consistent with Trp93 mediating hole hopping between the two hemes, in which the initial transient Fe(V) equivalent formed on the high-spin heme oxidizes Trp93, which in turn oxidizes the low-spin heme to yield the *bis*-Fe(IV) species.

Acknowledgments

This review was supported by NIH grants GM-41574 (VLD) and GM-66569 (CMW). The authors thank Erik Yukl for help in preparing Figures 2, 7, 8 and 9.

Acronyms and definitions

MADH	methylamine dehydrogenase, a periplasmic enzyme found in some gram-negative methylotrophic and autotrophic bacteria.
TTQ	the tryptophan tryptophylquinone enzyme cofactor consists of two Trp covalently cross-linked, with two keto groups added to one Trp.
Quinone	a benzene derivative in which two ring C-H have been replaced by C=O (diketobenzene derivative).
PreMADH	precursor form of methylamine dehydrogenase that is the substrate for MauG containing a monohydroxylated Trp.
Diferrous MauG	MauG in which both hemes are in the Fe(II) redox state.
Diferric MauG	MauG in which both hemes are in the Fe(III) redox state.

High-spin heme	where the iron retains its unpaired electrons upon axial coordination, indicative of weak ligand(s) binding.
Low-spin heme	where the iron has fewer unpaired electrons upon axial coordination, indicative of strong ligand(s) binding.
PreTTQ	precursor form of the tryptophan tryptophylquinone cofactor in which one –OH group has been added to one Trp.
UpPro and downPro	The two puckered forms of the prolyl ring (direction of Cβ and Cγ displacement from the mean ring plane), and defined by the endocyclic dihedral angles (45).
UpPro	χ0 ~ +6° (Cβ–Cα–N–Cδ), χ1 ~ −28° (N–Cα–Cβ–Cγ), χ2 ~ +39° (Cα –Cβ–Cγ–Cδ), χ3 ~-35° (Cβ–Cγ–C––N), χ4 ~ +18° (Cγ–Cδ–N–Cα). **DownPro**: χ0 ~ −10° (Cβ–Cα–N–Cδ), χ1 ~ +27° (N–Cα–Cβ–Cγ), χ2 ~ −36° (Cα–Cβ–Cγ–Cδ), χ3 ~ +29° (Cβ–Cγ–Cδ–N), χ4 ~ −12° (Cγ –Cδ–N–Cα).
Bis-Fe(IV) MauG	Fe(V)-equivalent redox state composed of a ferryl (Fe(IV)=O) heme and an Fe(IV) heme with two amino acid axial ligands.
Compound I	Fe(V)-equivalent redox state composed of ferryl (Fe(IV)=O) heme with a porphyrin cation radical.
Quinol	a benzene derivative in which two ring C-H have been replaced by C-OH (dihydroxybenzene derivative).
Random order kinetic mechanism	a catalytic reaction in which the order of addition of substrates to the reaction mix does not matter.
Ordered kinetic mechanism	a catalytic reaction in which one substrate must bind or react before another for catalysis to occur.
Electron tunneling	a single-step charge transfer process dependent on donor/acceptor composition and environment, distance and composition of the intervening medium.
Hole hopping in proteins	a multi-step charge transfer process in which single electron tunneling events occur concurrently through oxidation of intervening amino acids.

References

1. Davidson VL. Protein-derived cofactors. Expanding the scope of post-translational modifications. Biochemistry. 2007; 46:5283–92. [PubMed: 17439161]
2. Davidson VL. Generation of protein-derived redox cofactors by posttranslational modification. Mol. Biosyst. 2011; 7:29–37. [PubMed: 20936199]
3. Davidson VL. Pyrroloquinoline quinone (PQQ) from methanol dehydrogenase and tryptophan tryptophylquinone (TTQ) from methylamine dehydrogenase. Adv. Protein Chem. 2001; 58:95–140. [PubMed: 11665494]

4. Husain M, Davidson VL. An inducible periplasmic blue copper protein from Paracoccus denitrificans. Purification, properties, and physiological role. J. Biol. Chem. 1985; 260:14626–9. [PubMed: 2997215]
5. McIntire WS, Wemmer DE, Chistoserdov A, Lidstrom ME. A new cofactor in a prokaryotic enzyme: tryptophan tryptophylquinone as the redox prosthetic group in methylamine dehydrogenase. Science. 1991; 252:817–24. [PubMed: 2028257]
6. Chen L, Doi M, Durley RC, Chistoserdov AY, Lidstrom ME, et al. Refined crystal structure of methylamine dehydrogenase from Paracoccus denitrificans at 1.75 A resolution. J. Mol. Biol. 1998; 276:131–49. [PubMed: 9514722]
7. Chen L, Durley R, Poliks BJ, Hamada K, Chen Z, et al. Crystal structure of an electron-transfer complex between methylamine dehydrogenase and amicyanin. Biochemistry. 1992; 31:4959–64. [PubMed: 1599920]
8. Chen L, Durley RC, Mathews FS, Davidson VL. Structure of an electron transfer complex: methylamine dehydrogenase, amicyanin, and cytochrome c551i. Science. 1994; 264:86–90. [PubMed: 8140419]
9. Husain M, Davidson VL. Characterization of two inducible periplasmic c-type cytochromes from Paracoccus denitrificans. J. Biol. Chem. 1986; 261:8577–80. [PubMed: 3013855]
10. Mure M. Tyrosine-derived quinone cofactors. Acc. Chem. Res. 2004; 37:131–9. [PubMed: 14967060]
11. Janes SM, Mu D, Wemmer D, Smith AJ, Kaur S, et al. A new redox cofactor in eukaryotic enzymes: 6-hydroxydopa at the active site of bovine serum amine oxidase. Science. 1990; 248:981–7. [PubMed: 2111581]
12. Floris, G.; Mondovi, B., editors. Copper Amine Oxidases: Structures, catalytic mechanisms, and roles in pathophysiology. CRC Press; Boca Raton, Florida: 2009.
13. Matsuzaki R, Fukui T, Sato H, Ozaki Y, Tanizawa K. Generation of the topa quinone cofactor in bacterial monoamine oxidase by cupric ion-dependent autooxidation of a specific tyrosyl residue. Febs Lett. 1994; 351:360–4. [PubMed: 8082796]
14. Cai D, Klinman JP. Evidence of a self-catalytic mechanism of 2,4,5-trihydroxyphenylalanine quinone biogenesis in yeast copper amine oxidase. J. Biol. Chem. 1994; 269:32039–42. [PubMed: 7798196]
15. Kagan HM, Li W. Lysyl oxidase: properties, specificity, and biological roles inside and outside of the cell. J. Cell. Biochem. 2003; 88:660–72. [PubMed: 12577300]
16. Bollinger JA, Brown DE, Dooley DM. The formation of lysine tyrosylquinone (LTQ) is a self-processing reaction. Expression and characterization of a drosophila lysyl oxidase. Biochemistry. 2005; 44:11708–14. [PubMed: 16128571]
17. Wang SX, Mure M, Medzihradszky KF, Burlingame AL, Brown DE, et al. A crosslinked cofactor in lysyl oxidase: redox function for amino acid side chains. Science. 1996; 273:1078–84. [PubMed: 8688089]
18. Datta S, Mori Y, Takagi K, Kawaguchi K, Chen ZW, et al. Structure of a quinohemoprotein amine dehydrogenase with an uncommon redox cofactor and highly unusual crosslinking. Proc. Natl. Acad. Sci. U.S.A. 2001; 98:14268–73. [PubMed: 11717396]
19. Satoh A, Kim JK, Miyahara I, Devreese B, Vandenberghe I, et al. Crystal structure of quinohemoprotein amine dehydrogenase from Pseudomonas putida - Identification of a novel quinone cofactor encaged by multiple thioether cross-bridges. J. Biol. Chem. 2002; 277:2830–4. [PubMed: 11704672]
20. Vandenberghe I, Kim JK, Devreese B, Hacisalihoglu A, Iwabuki H, et al. The covalent structure of the small subunit from Pseudomonas putida amine dehydrogenase reveals the presence of three novel types of internal cross-linkages, all involving cysteine in a thioether bond. J. Biol. Chem. 2001; 276:42923–31. [PubMed: 11555656]
21. Wang Y, Graichen ME, Liu A, Pearson AR, Wilmot CM, Davidson VL. MauG, a novel diheme protein required for tryptophan tryptophylquinone biogenesis. Biochemistry. 2003; 42:7318–25. [PubMed: 12809487]

22. Chistoserdov AY, Boyd J, Mathews FS, Lidstrom ME. The genetic organization of the mau gene cluster of the facultative autotroph Paracoccus denitrificans. Biochem. Biophys. Res. Commun. 1992; 184:1181–9. [PubMed: 1590782]

23. van der Palen CJ, Slotboom DJ, Jongejan L, Reijnders WN, Harms N, et al. Mutational analysis of mau genes involved in methylamine metabolism in Paracoccus denitrificans. Eur. J. Biochem. 1995; 230:860–71. [PubMed: 7601147]

24. van Spanning RJ, Wansell CW, Reijnders WN, Oltmann LF, Stouthamer AH. Mutagenesis of the gene encoding amicyanin of Paracoccus denitrificans and the resultant effect on methylamine oxidation. Febs Lett. 1990; 275:217–20. [PubMed: 2261991]

25. Chistoserdov AY, Chistoserdova LV, Mcintire WS, Lidstrom ME. Genetic organization of the mau gene cluster in Methylobacterium extorquens Am1. Complete nucleotide sequence and generation and characteristics of mau mutants. J. Bacteriol. 1994; 176:4052–65. [PubMed: 8021187]

26. van der Palen CJ, Reijnders WN, de Vries S, Duine JA, van Spanning RJ. MauE and MauD proteins are essential in methylamine metabolism of Paracoccus denitrificans. Antonie van Leeuwenhoek. 1997; 72:219–28. [PubMed: 9403107]

27. Husain M, Davidson VL. Purification and properties of methylamine dehydrogenase from Paracoccus denitrificans. J Bacteriol. 1987; 169:1712–7. [PubMed: 3558322]

28. Graichen ME, Jones LH, Sharma BV, van Spanning RJ, Hosler JP, Davidson VL. Heterologous expression of correctly assembled methylamine dehydrogenase in Rhodobacter sphaeroides. J. Bacteriol. 1999; 181:4216–22. [PubMed: 10400578]

29. Pearson AR, de la Mora-Rey T, Graichen ME, Wang Y, Jones LH, et al. Further insights into quinone cofactor biogenesis: Probing the role of MauG in methylamine dehydrogenase TTQ formation. Biochemistry. 2004; 43:5494–502. [PubMed: 15122915]

30. Pearson AR, Marimanikkuppam S, Li X, Davidson VL, Wilmot CM. Isotope labeling studies reveal the order of oxygen incorporation into the tryptophan tryptophylquinone cofactor of methylamine dehydrogenase. J. Am. Chem. Soc. 2006; 128:12416–7. [PubMed: 16984182]

31. Wang Y, Li X, Jones LH, Pearson AR, Wilmot CM, Davidson VL. MauG-dependent in vitro biosynthesis of tryptophan tryptophylquinone in methylamine dehydrogenase. J. Am. Chem. Soc. 2005; 127:8258–9. [PubMed: 15941239]

32. Davidson VL, Brooks HB, Graichen ME, Jones LH, Hyun YL. Detection of intermediates in tryptophan tryptophylquinone enzymes. Methods Enzymol. 1995; 258:176–90. [PubMed: 8524149]

33. Li X, Fu R, Liu A, Davidson VL. Kinetic and physical evidence that the di-heme enzyme MauG tightly binds to a biosynthetic precursor of methylamine dehydrogenase with incompletely formed tryptophan tryptophylquinone. Biochemistry. 2008; 47:2908–12. [PubMed: 18220357]

34. Li X, Jones LH, Pearson AR, Wilmot CM, Davidson VL. Mechanistic possibilities in MauG-dependent tryptophan tryptophylquinone biosynthesis. Biochemistry. 2006; 45:13276–83. [PubMed: 17073448]

35. Shin S, Abu Tarboush N, Davidson VL. Long range electron transfer reactions between hemes of MauG and different forms of tryptophan tryptophylquinone of methylamine dehydrogenase. Biochemistry. 2010; 49:5810–6. [PubMed: 20540536]

36. Li X, Feng M, Wang Y, Tachikawa H, Davidson VL. Evidence for redox cooperativity between c-type hemes of MauG which is likely coupled to oxygen activation during tryptophan tryptophylquinone biosynthesis. Biochemistry. 2006; 45:821–8. [PubMed: 16411758]

37. Li X, Fu R, Lee S, Krebs C, Davidson VL, Liu A. A catalytic di-heme bis-Fe(IV)intermediate, alternative to an Fe(IV)=O porphyrin radical. Proc. Natl. Acad. Sci. U.S.A. 2008; 105:8597–600. [PubMed: 18562294]

38. Lee S, Shin S, Li X, Davidson VL. Kinetic mechanism for the initial steps in MauG-dependent tryptophan tryptophylquinone biosynthesis. Biochemistry. 2009; 48:2442–7. [PubMed: 19196017]

39. Jensen LM, Sanishvili R, Davidson VL, Wilmot CM. In crystallo posttranslational modification within a MauG/pre-methylamine dehydrogenase complex. Science. 2010; 327:1392–4. [PubMed: 20223990]

40. Jensen LMR, Meharenna YT, Davidson VL, Poulos TL, Hedman B, et al. Geometric and electronic structures of the His-Fe(IV)=O and His-Fe(IV)-Tyr hemes of MauG. J. Biol. Inorg. Chem. 2012 in press.
41. Shin S, Feng ML, Chen Y, Jensen LMR, Tachikawa H, et al. The tightly bound calcium of MauG is required for tryptophan tryptophylquinone cofactor biosynthesis. Biochemistry. 2011; 50:144–50. [PubMed: 21128656]
42. Fu R, Liu F, Davidson VL, Liu A. Heme iron nitrosyl complex of MauG reveals an efficient redox equilibrium between hemes with only one heme exclusively binding exogenous ligands. Biochemistry. 2009; 48:11603–5. [PubMed: 19911786]
43. Yukl ET, Goblirsch BR, Davidson VL, Wilmot CM. Crystal structures of CO and NO adducts of MauG in complex with pre-methylamine dehydrogenase: Implications for the mechanism of dioxygen activation. Biochemistry. 2011; 50:2931–8. [PubMed: 21355604]
44. Ling Y, Davidson VL, Zhang Y. Unprecedented Fe(IV) species in a diheme protein MauG: A quantum chemical investigation on the unusual Mössbauer spectroscopic properties. J. Phys. Chem. Lett. 2010; 1:2936–9. [PubMed: 20953337]
45. Nemethy G, Gibson KD, Palmer KA, Yoon CN, Paterlini G, et al. Energy parameters in polypeptides 10. Improved geometrical parameters and nonbonded interactions for use in the ECEPP/3 algorithm, with application to proline-containing peptides. J. Phys. Chem. 1992; 96:6472–84.
46. Feng M, Jensen LM, Yukl ET, Wei X, Liu A, et al. Proline 107 Is a major determinant in maintaining the structure of the distal pocket and reactivity of the high-spin heme of MauG. Biochemistry. 2012; 51:1598–606. [PubMed: 22299652]
47. Chen Y, Naik SG, Krzystek J, Shin S, Nelson WH, et al. Role of calcium in metalloenzymes: Effects of calcium removal on the axial ligation geometry and magnetic properties of the catalytic diheme center in MauG. Biochemistry. 2012; 51:1586–97. [PubMed: 22320333]
48. Walker FA. Magnetic spectroscopic (EPR, ESEEM, Mössbauer, MCD and NMR) studies of low-spin ferriheme centers and their corresponding heme proteins. Coord. Chem. Rev. 1999; 185-186:471–534.
49. Zoppellaro G, Bren KL, Ensign AA, Harbitz E, Kaur R, et al. Review: studies of ferric heme proteins with highly anisotropic/highly axial low spin (S = 1/2) electron paramagnetic resonance signals with bis-histidine and histidine-methionine axial iron coordination. Biopolymers. 2009; 91:1064–82. [PubMed: 19536822]
50. Jones LH, Pearson AR, Tang Y, Wilmot CM, Davidson VL. Active site aspartate residues are critical for tryptophan tryptophylquinone biogenesis in methylamine dehydrogenase. J. Biol. Chem. 2005; 280:17392–6. [PubMed: 15734739]
51. Meunier B, de Visser SP, Shaik S. Mechanism of oxidation reactions catalyzed by cytochrome P450 enzymes. Chem Rev. 2004; 104:3947–80. [PubMed: 15352783]
52. Shin S, Lee S, Davidson VL. Suicide inactivation of MauG during reaction with O_2 or H_2O_2 in the absence of its natural protein substrate. Biochemistry. 2009; 48:10106–12. [PubMed: 19788236]
53. Husain M, Davidson VL, Gray KA, Knaff DB. Redox properties of the quinoprotein methylamine dehydrogenase from Paracoccus denitrificans. Biochemistry. 1987; 26:4139–43. [PubMed: 3651442]
54. Abu Tarboush N, Jensen LM, Feng M, Tachikawa H, Wilmot CM, Davidson VL. Functional importance of tyrosine 294 and the catalytic selectivity for the bis-Fe(IV) state of MauG revealed by replacement of this axial heme ligand with histidine. Biochemistry. 2010; 49:9783–91. [PubMed: 20929212]
55. Gray HB, Winkler JR. Electron tunneling through proteins. Q. Rev. Biophys. 2003; 36:341–72. [PubMed: 15029828]
56. Giese B, Graber M, Cordes M. Electron transfer in peptides and proteins. Curr. Opin. Chem. Biol. 2008; 12:755–9. [PubMed: 18804174]
57. Abu Tarboush N, Jensen LMR, Yukl ET, Geng J, Liu A, et al. Mutagenesis of tryptophan199 suggets that hopping is required for MauG-dependent tryptophan tryptophylquinone biosynthesis. Proc. Natl. Acad. Sci. U.S.A. 2011; 108:16956–61. [PubMed: 21969534]

58. Choi M, Shin S, Davidson VL. Characterization of electron tunneling and hole hopping reactions between different forms of MauG and methylamine dehydrogenase within a natural protein complex. Biochemistry. 2012; 51:6942–9. [PubMed: 22897160]

Summary points

1. TTQ is one example in a growing family of protein-derived cofactors which result from post-translational modifications that transform active site amino acids into redox and catalytic centers.
2. TTQ is biosynthesized from two Trp residues in the active site of MADH, and requires the insertion of two oxygens into one of the indole rings and cross-linking of the two Trp residues.
3. MauG is a *c*-type diheme enzyme that completes TTQ biosynthesis. The substrate for MauG is preMADH that already contains a monohydroxylated Trp (preTTQ), and so MauG catalyzes the final six-electron oxidation.
4. One MauG heme is high-spin five-coordinate, and the other heme is low-spin with an unusual His-Tyr axial ligation (the first observed for a *c*-type heme). The reduction potentials of the two hemes are similar, and facile electron transfer between them occurs via a conserved Trp93, meaning that the diheme unit acts as a single redox cofactor.
5. The potent, catalytically competent MauG oxidant is an unprecedented *bis*-Fe(IV) redox state that is long-lived compared to other Fe(V)-equivalent species.
6. The axial Tyr294 ligand to the low-spin heme is key to attaining the *bis*-Fe(IV) state, and a His variant at this position could not catalyze TTQ formation.
7. The post-translational modifications occur ~ 40 Å from the site of H_2O_2 / O_2 binding, and ~ 15 Å from the diheme unit. The electron transfer from preTTQ to the *bis*-Fe(IV) of MauG requires MauG Trp199, which is transiently and reversibly oxidized to a radical during electron transfer in a hole hopping mechanism, in contrast to the more usual electron tunneling that operates over shorter distances.

Future Issues

1. How is the first hydroxyl group added to the MADH Trp prior to MauG catalysis?
2. What is the order of the three two-electron oxidation events in the MauG catalyzed post-translational modification?
3. What is the precise nature of the radical intermediates that precede the crosslinking and oxygenation reactions?
4. What can we learn about oxidative damage mechanisms caused by highly reactive oxidizing species through the study of the long-lived MauG *bis*-Fe(IV)?
5. How do the same preMADH residues around preTTQ contribute to the different chemistries that occur during TTQ biosynthesis?

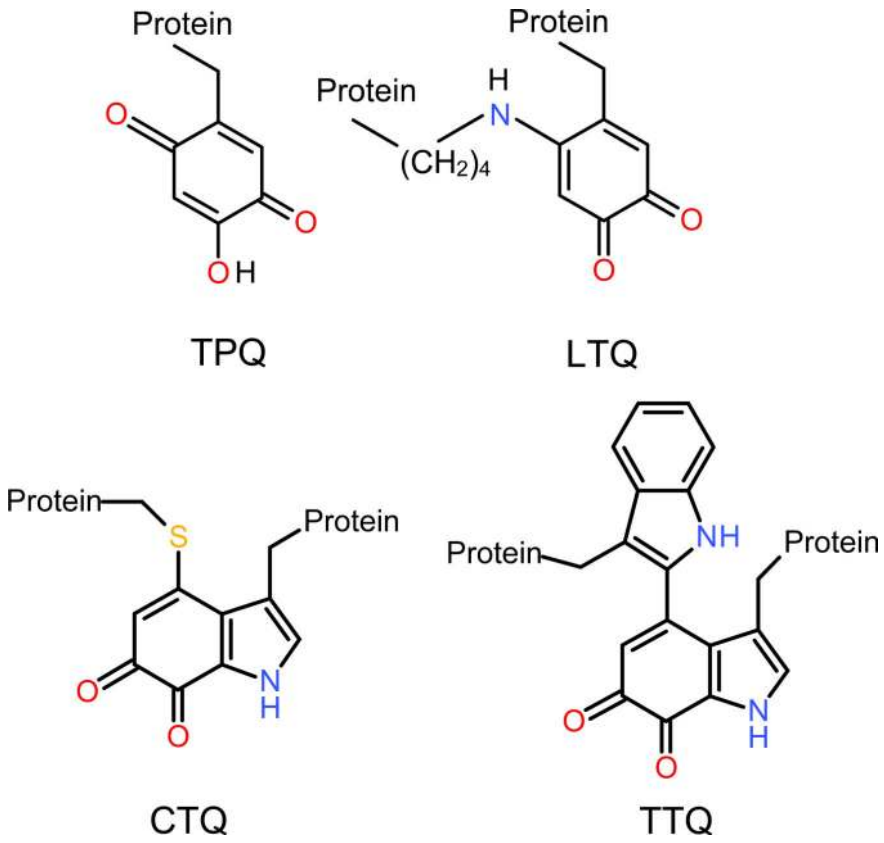

Figure 1.
Protein-derived quinone cofactors. TPQ, 2,4,5-trihydroxyphenylalanine quinone; LTQ, lysine tyrosylquinone; CTQ, cysteine tryptophylquinone; TTQ, tryptophan tryptophylquinone.

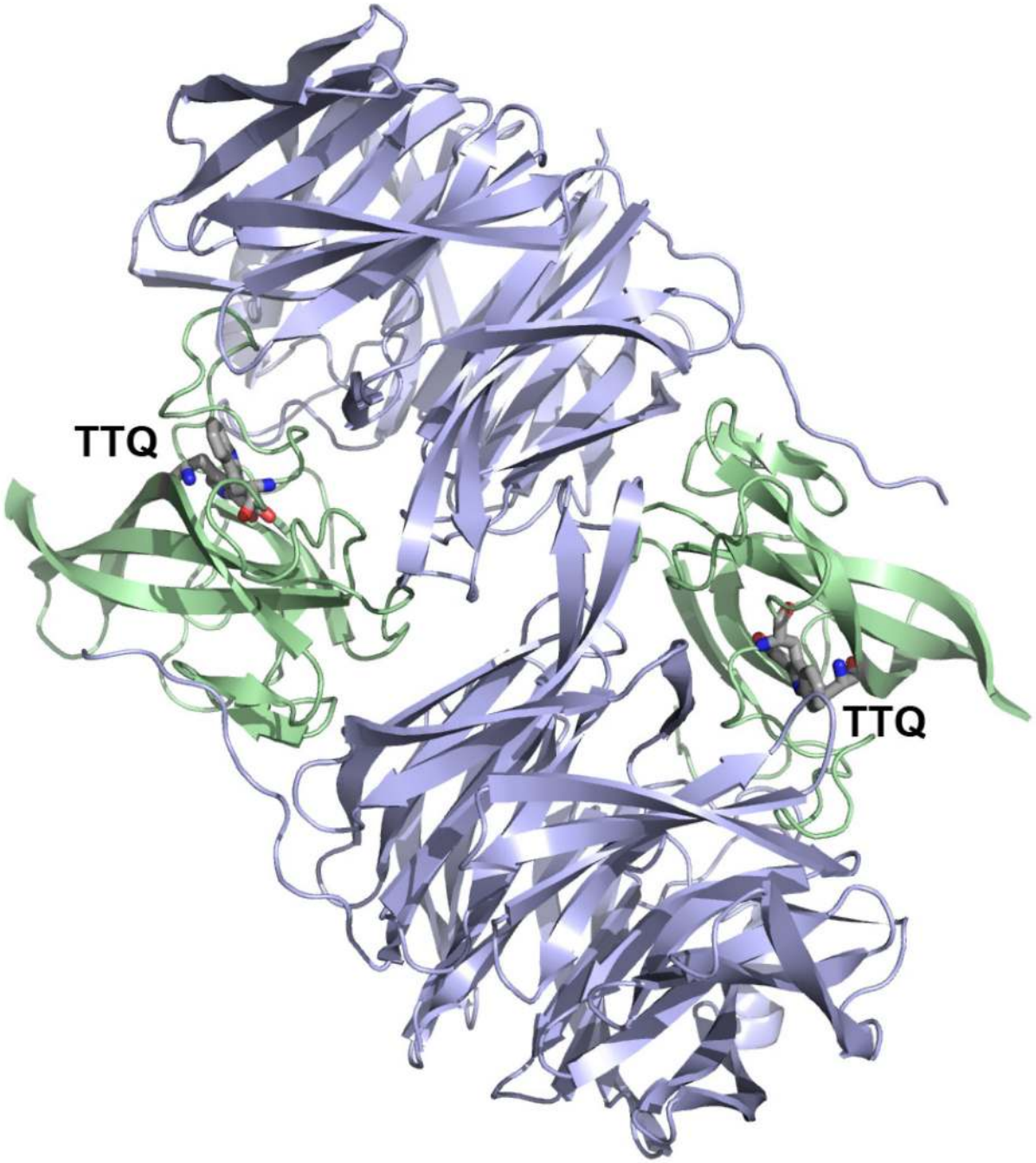

Figure 2.

Crystal structure of methylamine dehydrogenase (MADH). The overall fold of MADH (PDB code: 2bbk) (6) is represented in cartoon (MADH α-subunit, blue; MADH β-subunit, green) with TTQ drawn in stick colored by atom. Figure produced using PyMOL (www.pymol.org).

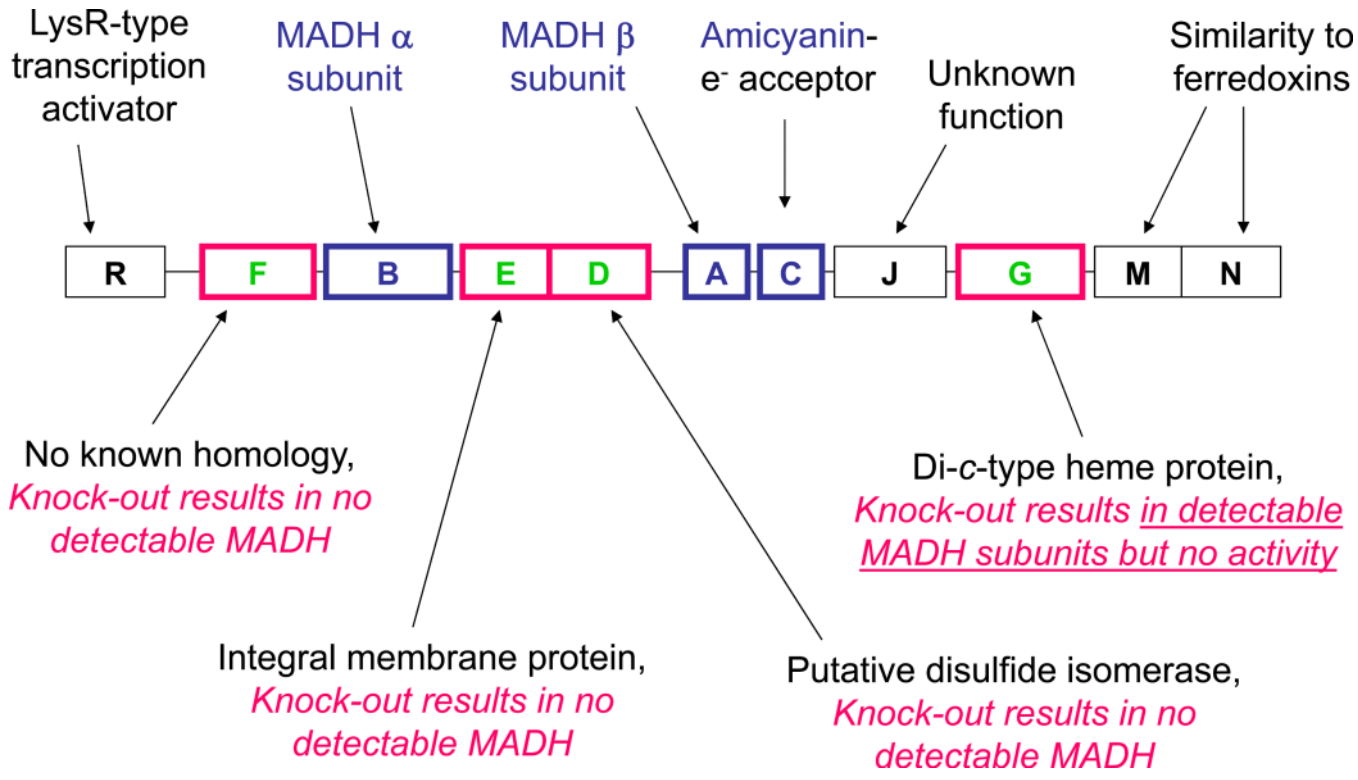

Figure 3.

The *mau* gene cluster of *P. denitrificans*. Of these genes only the gene products of *mauB, mauA, mauC* and *mauG* have been isolated and characterized. For the other genes assignment of structure or function is based on sequence similarity to other genes of known function. The information in this figure is based on data presented in references (23, 24, 26).

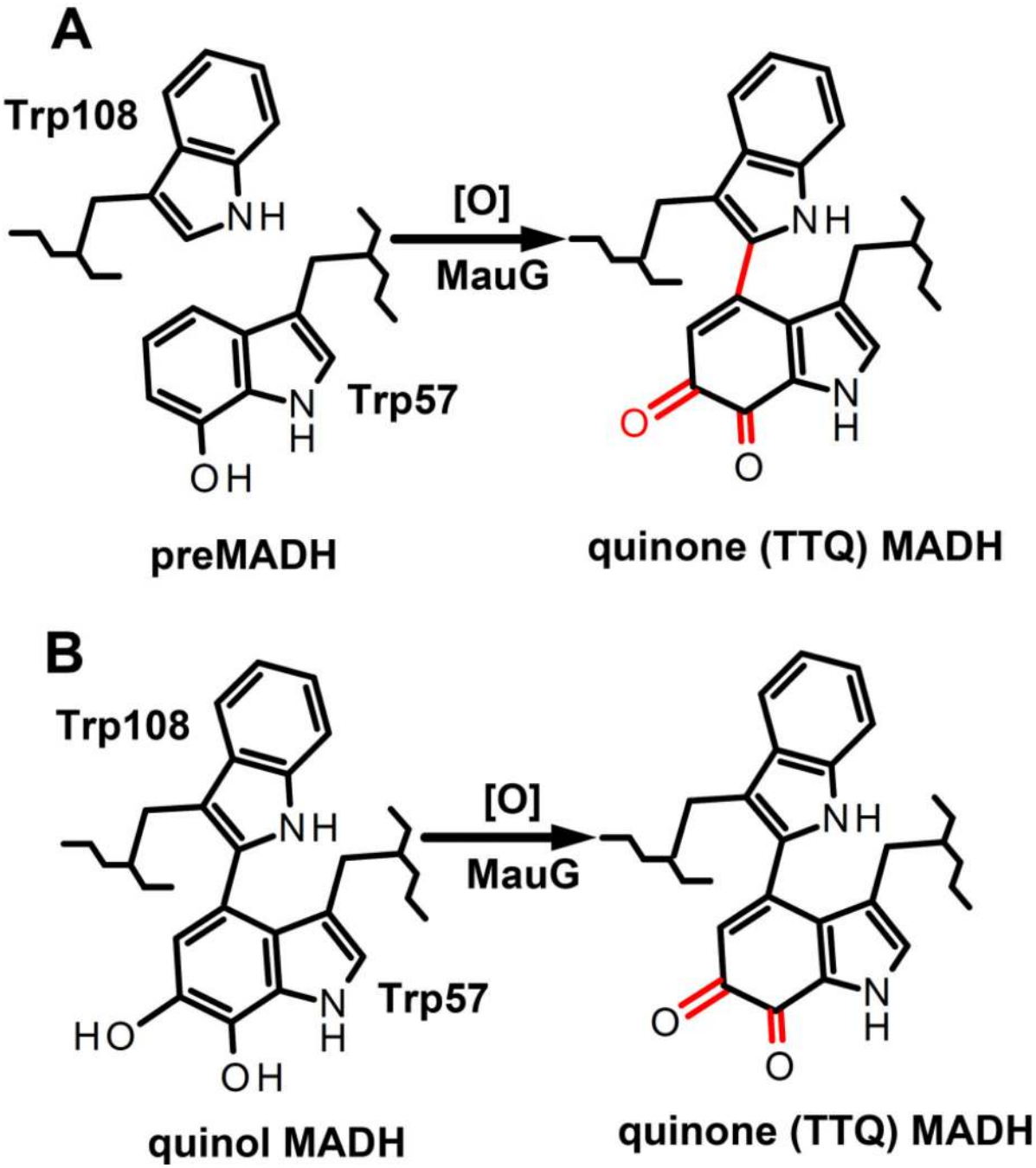

Figure 4.

Reactions catalyzed by MauG that have been monitored by steady-state kinetics. (A) MauG-dependent TTQ biosynthesis from preMADH. (B) MauG-dependent oxidation of reduced quinol MADH to TTQ.

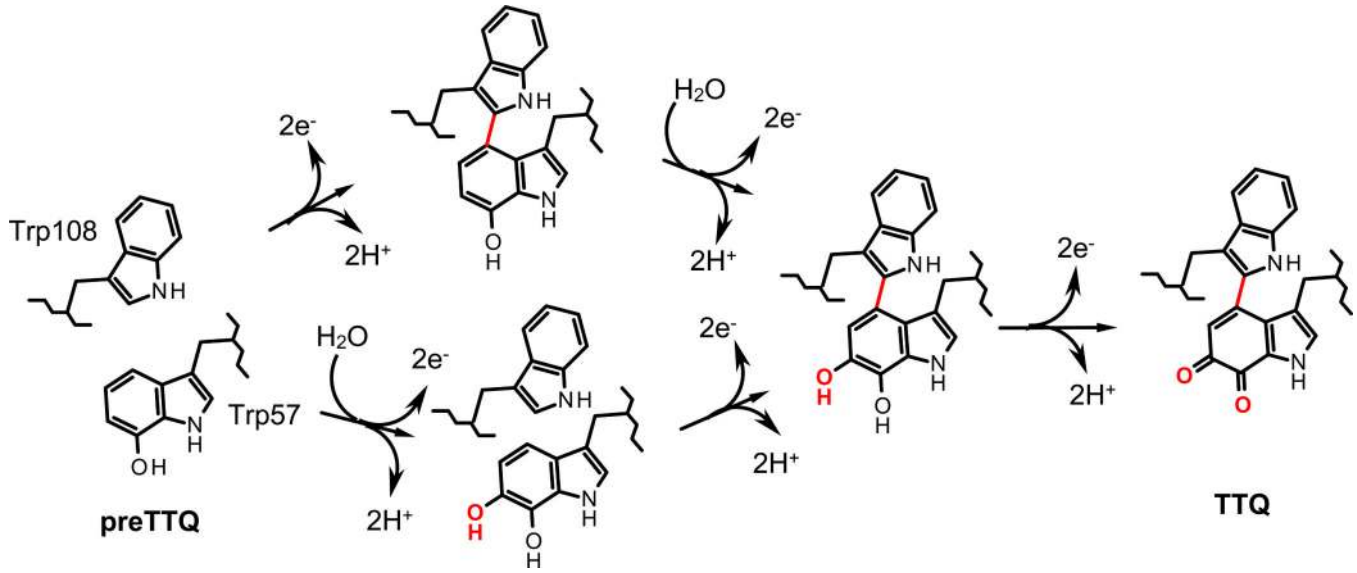

Figure 5.

A model for MauG-dependent TTQ biosynthesis from preMADH. As the order of the cross-linking and hydroxylation steps are not known, the two alternative possible routes to form the quinol TTQ are presented. The post-translational modifications are shown in red.

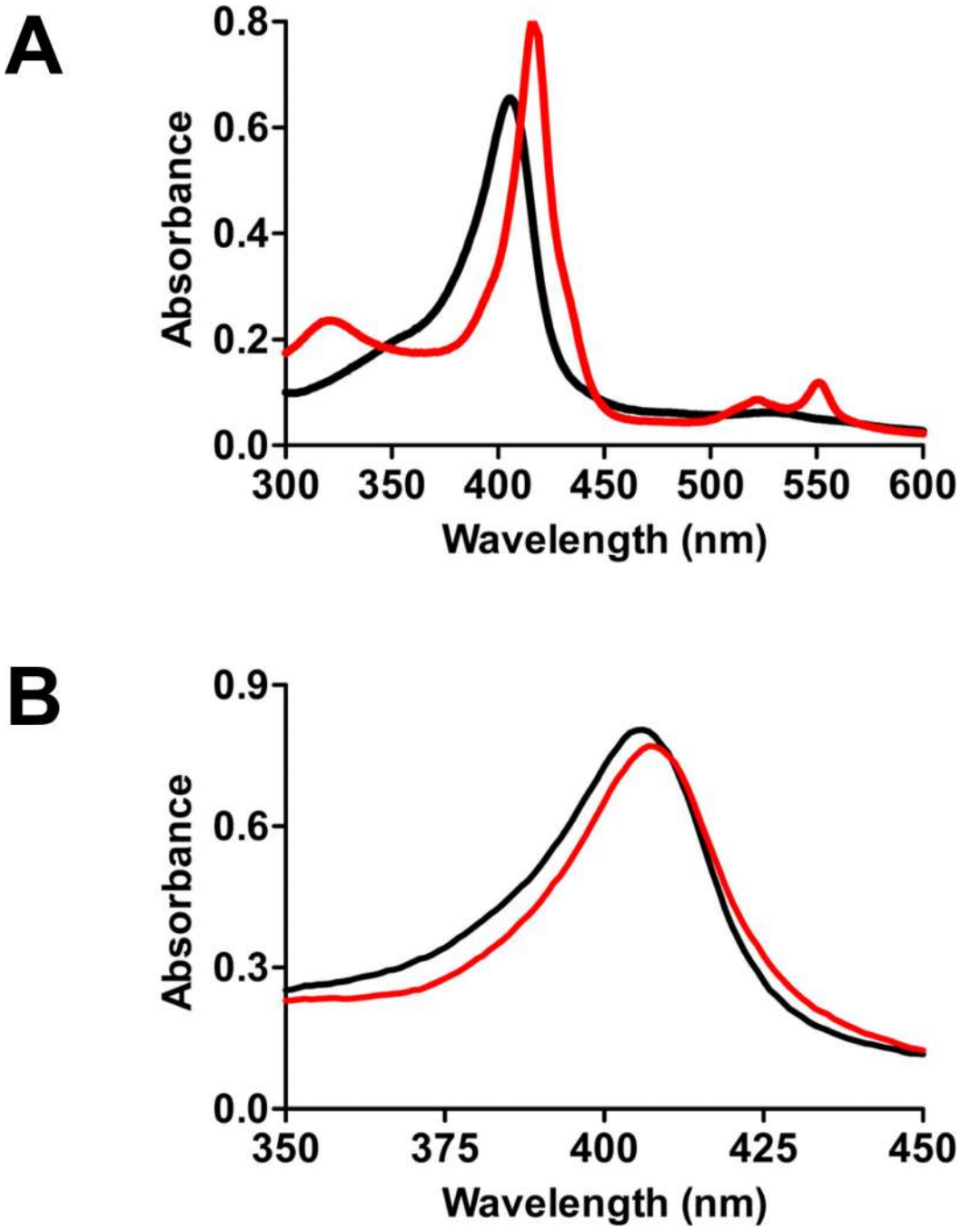

Figure 6.
UV-visible absorption spectra of different redox states of MauG. (A) diferric (black) and diferrous (red). (B) Diferric (black) and *bis*-Fe(IV) (red).

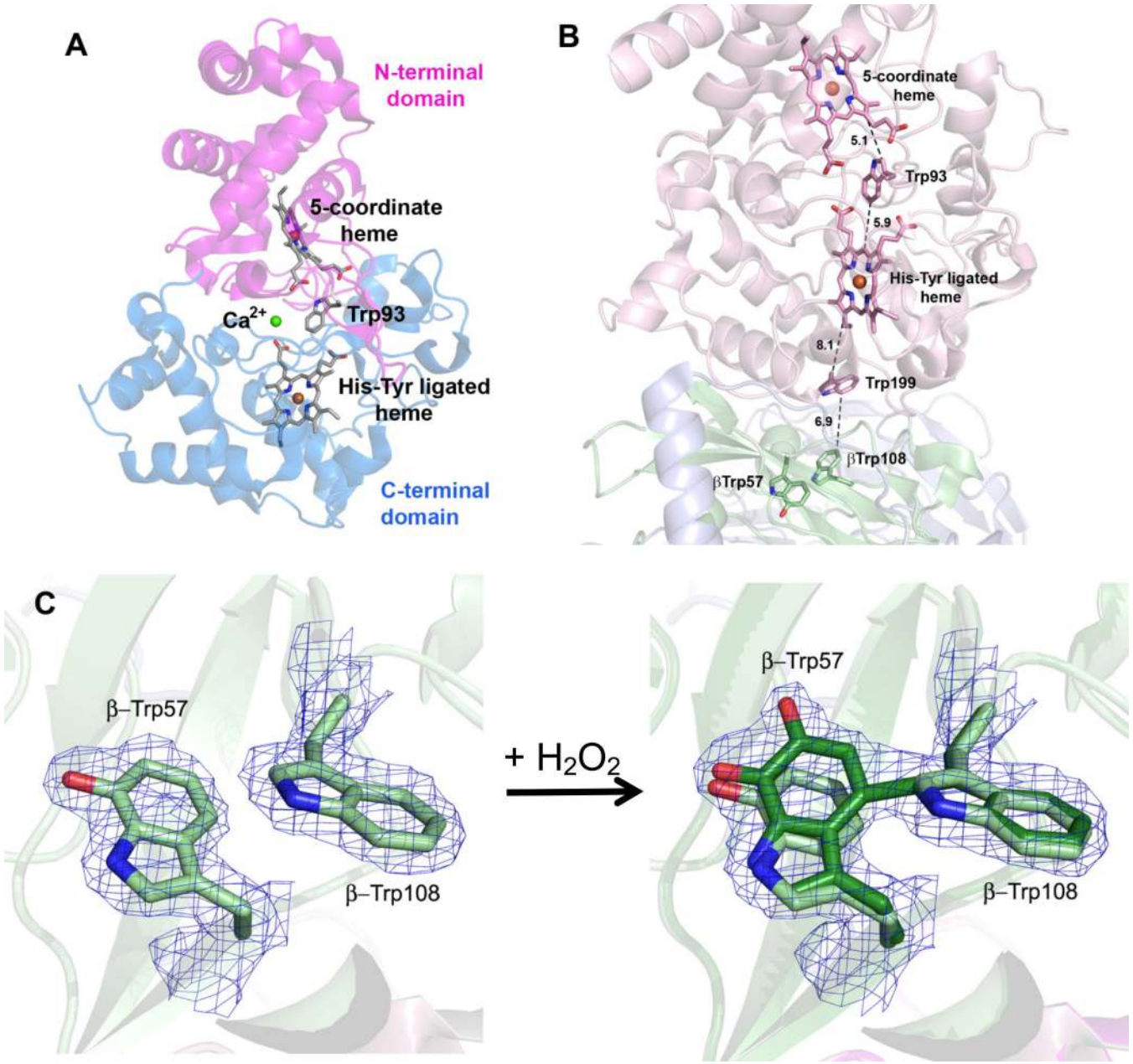

Figure 7.

Crystal structures of MauG in complex with precursor methylamine dehydrogenase (preMADH). (A) Overall fold of MauG colored by domain (PDB code: 3l4m) (39). (B) Key components of electron transfer between preMADH and MauG. (C) PreTTQ site before (left panel) and after (right panel) addition of H_2O_2 to MauG-preMADH crystals (PDB codes: 3l4m (left) and 3l4o (right)). The proteins are represented in cartoon (MADH α-subunit, blue; MADH β-subunit, green; panel (B), MauG, pink). Hemes, Trps, TTQ and preTTQ drawn in stick colored by atom (panel (B), carbon, color of associated protein chain cartoon; panel (C), preTTQ, light green, TTQ, dark green). Irons and calcium are drawn as orange

and green spheres, respectively. 2Fo-Fc electron density (blue) contoured at 1.0σ. Figure produced using PyMOL (www.pymol.org).

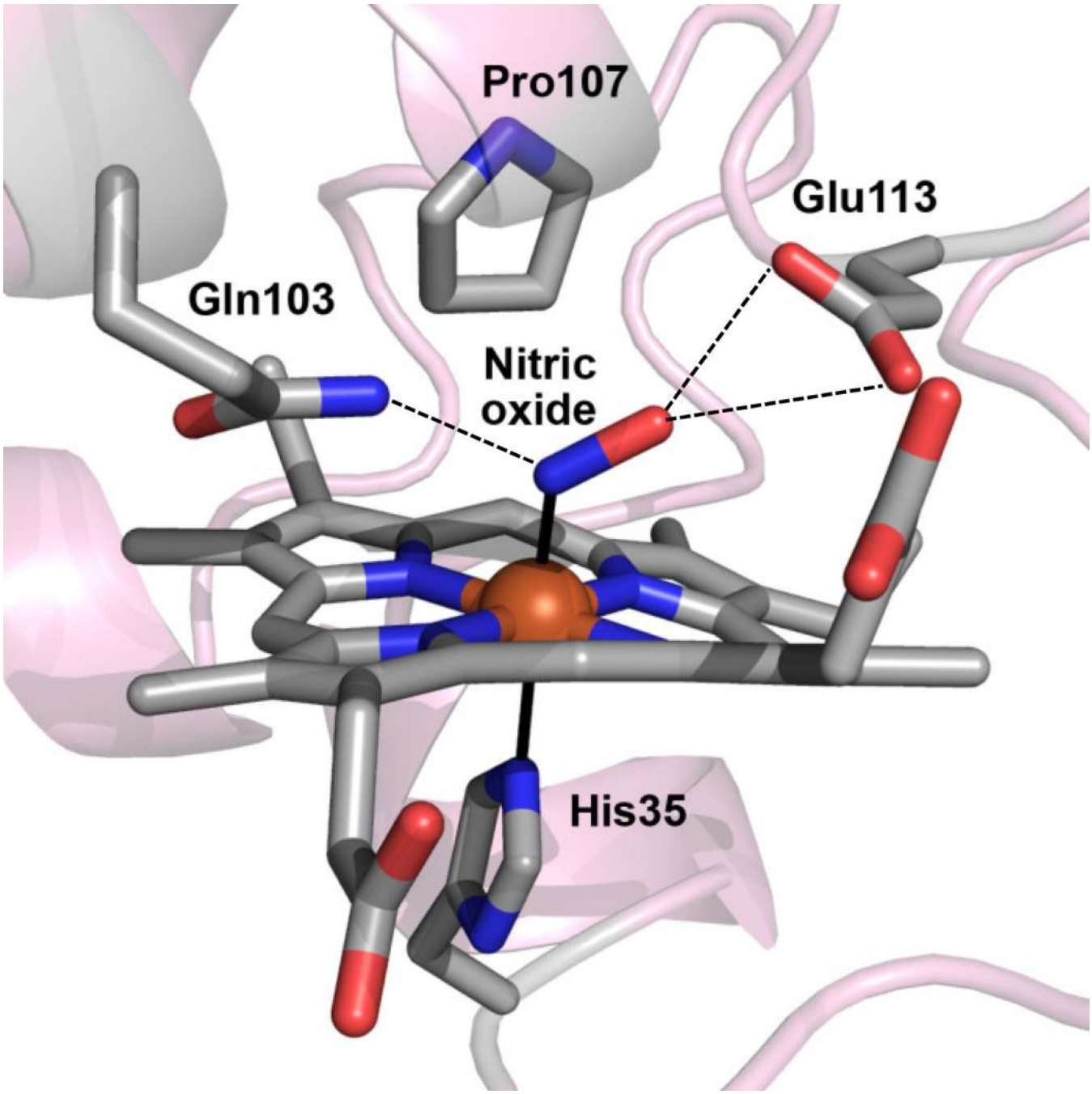

Figure 8.
Crystal structure of nitric oxide in complex with diferrous MauG-preMADH (PDB code: 2pxw) (43). NO binds to the heme that lies furthest from the MauG-preMADH interface. Colors and representation are as in Figure 7. Hydrogen bonds are indicated by dashed lines. Figure produced using PyMOL (www.pymol.org).

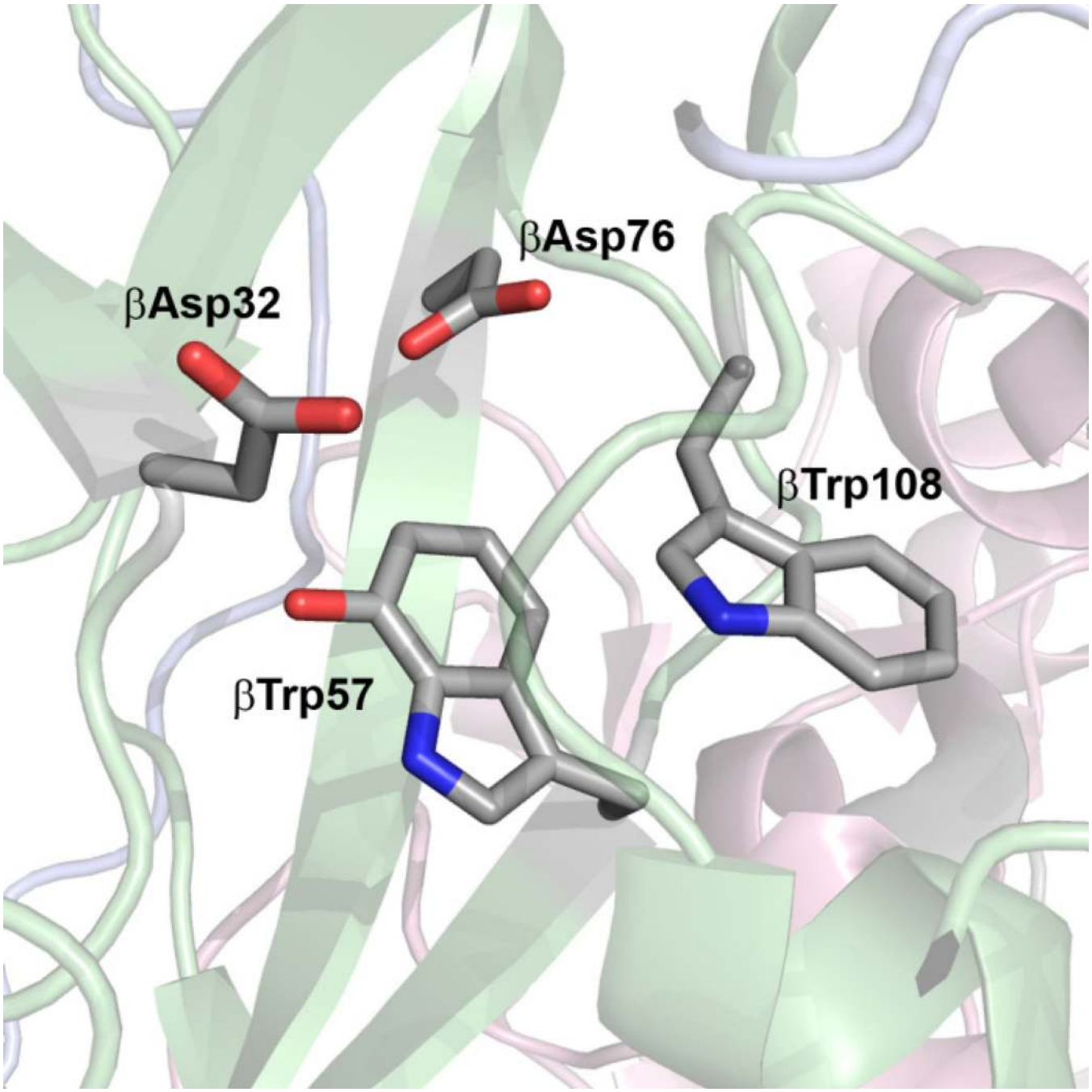

Figure 9.
The preTTQ site of the preMADH β subunit showing Asp residues that are critical for the hydroxylation of βTrp57 to form preTTQ (PDB code: 3l4m) (39). Colors and representation are as in Figure 7. Figure produced using PyMOL (www.pymol.org).

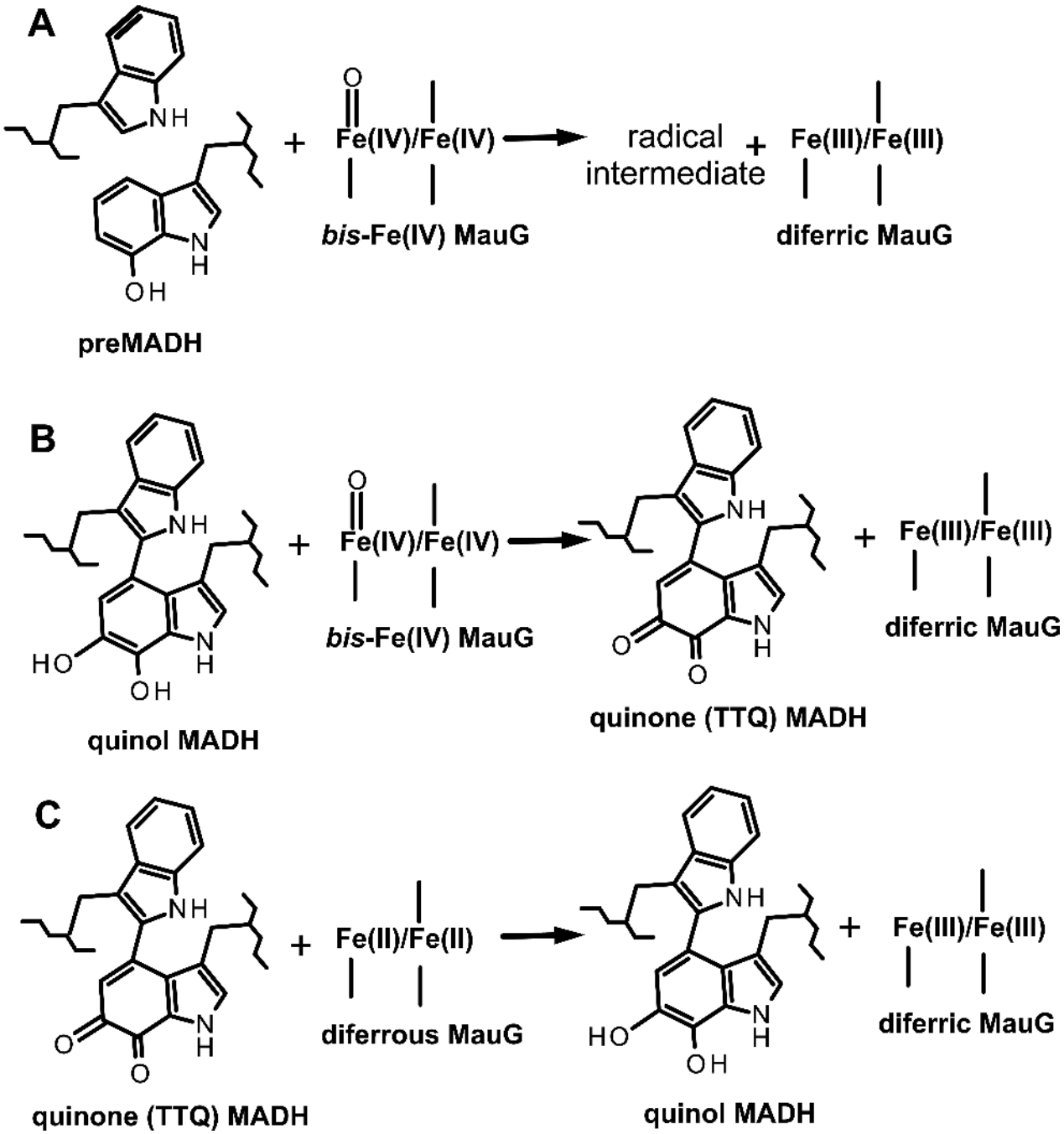

Figure 10.

Electron transfer reactions that have been characterized by single-turnover kinetics. (A) The initial two-electron oxidation step in TTQ biosynthesis from preMADH to *bis*-Fe(IV) MauG. (B) The final two-electron oxidation step in TTQ biosynthesis from quinol MADH to *bis*-Fe(IV) MauG. (C) The non-biosynthetic electron transfer reaction from diferrous MauG to quinone MADH.

Table 1

Kinetic parameters for steady-state and single turnover reactions.

Steady state TTQ formation from preMADH	
k_{cat} (s^{-1})	0.20 ± 0.01
K_m (μM)	6.6 ± 0.6
Steady state TTQ formation from quinol MADH	
k_{cat} (s^{-1})	4.2 ± 0.2
K_m (μM)	11.1 ± 1.3
Electron transfer from preMADH to *bis*-Fe(IV) MauG	
k (s^{-1})	0.8 ± 0.1
K_d (μM)	≤1.5
Electron transfer from quinol MADH to *bis*-Fe(IV) MauG	
k (s^{-1})	20 ± 1.3
K_d (μM)	11.2 ± 2.3
Electron transfer from diferrous MauG to quinone MADH	
k (s^{-1})	0.07 ± 0.01
K_d (μM)	10.1 ± 1.6

Data are taken from references (34, 35, 38)